JACC: ADVANCES VOL. 3, NO. 7, 2024

ORIGINAL RESEARCH

CONGENITAL HEART DISEASE

Multiphysiologic State Computational Fluid Dynamics Modeling for Planning Fontan With Interrupted Inferior Vena Cava

David M. Hoganson, MD,[a] Vijay Govindarajan, PhD,[a] Noah E. Schulz, MS,[a] Emily R. Eickhoff, MS,[a] Roger E. Breitbart, MD,[b] Gerald R. Marx, MD,[b] Pedro J. del Nido, MD,[a] Peter E. Hammer, PhD[a]

ABSTRACT

BACKGROUND Single ventricle (SV) patients with interrupted inferior vena cava (iIVC) and azygos continuation are at high risk for unbalanced hepatic venous flow (HVF) distribution to the lungs after Fontan completion and subsequent pulmonary arteriovenous malformations (AVMs) formation.

OBJECTIVES The aim of the study was to utilize computational fluid dynamics (CFD) analysis to avoid maldistribution of HVF to the lungs after Fontan surgery.

METHODS Four SV subjects with iIVC were prospectively studied with a 3-dimensional (3D) modeling workflow with digital 3D models created from segmented magnetic resonance images or computer tomography scans, virtual surgery, and CFD analysis over multiple physiologic states for the evaluation of operative plans to achieve balanced HVF to both lungs. Three of the patients were Fontan revision candidates with existing AVMs. All patients underwent Fontan completion or revision surgery.

RESULTS CFD predicted that existing or proposed Fontan completion in all patients would result in 100% of HVF to one lung. Improved HVF balance was achieved with CFD analysis of alternative surgical approaches resulting in the average distribution of HVF to the right/left pulmonary arteries of 37%/63% ± 10.4%. A hepatoazygos shunt was required in all patients and additional creation of an innominate vein in one. CFD analysis was validated by the comparison of pre-operative predicted and postoperative MRI-measured total right/left pulmonary flow (51%/49% ± 5.4% vs 49%/51% ± 8.5%).

CONCLUSIONS A 3D modeling workflow with CFD simulation for SV patients with iIVC may avoid HVF maldistribution and development of AVMs after Fontan completion. (JACC Adv 2024;3:101057) © 2024 The Authors. Published by Elsevier on behalf of the American College of Cardiology Foundation. This is an open access article under the CC BY-NC-ND license (http://creativecommons.org/licenses/by-nc-nd/4.0/).

From the [a]Department of Cardiac Surgery, Boston Children's Hospital, Boston, Massachusetts, USA; and the [b]Department of Cardiology, Boston Children's Hospital, Boston, Massachusetts, USA.

The authors attest they are in compliance with human studies committees and animal welfare regulations of the authors' institutions and Food and Drug Administration guidelines, including patient consent where appropriate. For more information, visit the Author Center.

Manuscript received October 9, 2023; revised manuscript received March 1, 2024, accepted April 21, 2024.

ISSN 2772-963X https://doi.org/10.1016/j.jacadv.2024.101057

ABBREVIATIONS AND ACRONYMS

3D = 3-dimensional

AVMs = pulmonary arteriovenous malformations

CFD = computational fluid dynamics

HA = hepatoazygos

HVF = hepatic venous flow

iIVC = interrupted inferior vena cava

IVC = inferior vena cava

SV = single ventricle

SVC = superior vena cava

In the Fontan circulation, balanced distribution of hepatic venous flow (HVF) into both lungs is essential for a favorable long-term outcome. The "hepatic factor" is a yet undetermined molecule, metabolite, or perhaps even lack of a hepatic factor that occurs in the hepatic venous blood that must be distributed to both lungs to prevent pulmonary arteriovenous malformations (AVMs). In patients with a single superior vena cava (SVC) and intact inferior vena cava (IVC) on the same side as the SVC, a lateral tunnel or extracardiac Fontan generally delivers a reasonable balance of HVF to both lungs, with AVMs occurring rarely. In contrast, patients with interrupted inferior vena cava (iIVC) and azygos continuation as part of heterotaxy/polysplenia syndrome present unique challenges to HVF distribution. These individuals appear to have an underlying propensity to form AVMs that develop in 32 to 85% of patients after Kawashima prior to the Fontan or within the first 5 years of life.[2-6] Resolution of the existing AVMs and prevention of new late AVMs is dependent upon balancing HVF to both lungs.

Many iIVC patients undergo Fontan completion with a lateral tunnel or extracardiac conduit to incorporate the HVF directly into the pulmonary arteries. If most or all of the HVF streams to one lung, AVMs can develop in the contralateral lung.[7-12] In Kawashima patients, surgically diverting the hepatic veins to the pulmonary arteries to ensure hepatic venous blood reaches both lungs involves predicting how blood from 3 or more inlets mixes and distributes itself across 2 outlets. The relationships among these multiple inflows and outflows vary with activity level and prandial state. These factors, coupled with the anatomical complexity in iIVC patients, results in wide variability in HVF distribution after Fontan completion even in the hands of experienced surgeons.

AVMs in iIVC patients were shown to resolve following hepatic vein incorporation into the pulmonary circulation with the creation of a hepatoazygos (HA) shunt, directing all of the HVF to the superior cavopulmonary connection via the azygos vein.[9,13] Other creative surgical approaches to achieve the same effective goal have been described including incorporation of the hepatic veins into the SVC via conduit[14] or into the innominate vein.[12]

To address the risk or presence of HVF maldistribution, several groups have used computational fluid dynamics (CFD) flow modeling to help plan Fontan completion.[8,11,15-23] Specifically addressing hepatic vein incorporation in SV patients with iIVC, Simulation predicted that the optimal solution depended on the specific anatomy and relative caval inflow rates, indicating the need for patient-specific modeling. This was underscored by Alsoufi et al[8] who showed that a significant proportion of patients who had surgery to address AVMs following the Kawashima procedure had persistent low SaO_2 on follow up, indicating incomplete resolution of AVMs.

In this study, we present our recent experience using CFD to aid in surgical planning for a series of 4 prospective patients with iIVC. Our workflow emphasized accurate modeling of the existing anatomy with detailed virtual surgery models created for different surgical options with performance of CFD, importantly in 4 different physiological conditions to understand the robustness of the flow balance over a range of physiological states shown in the **Central Illustration**.

METHODS

Four subjects with SV and iIVC were evaluated prospectively with 3-dimensional (3D) modeling and CFD to quantitatively predict and evaluate the operative plan for achieving balanced HVF to both lungs. The anatomic and clinical characteristics of the patients are shown in **Table 1**. AVMs were diagnosed in the catheterization lab by transit time of pulmonary artery flow, typical speckled appearance by angiography, and corresponding low oxygen saturations of individual pulmonary veins. Institutional Review Board approval was obtained.

3D MODELING WORKFLOW WITH VIRTUAL SURGERY TO CREATE PATIENT-SPECIFIC FONTAN COMPLETION MODELS. A workflow was developed for these patients (**Figure 1**) that started with the segmentation of a cardiac MRI or CT scan utilizing Mimics software (Materialise NV) to create a patient-specific 3D model of the existing anatomy. These models include the left (when present) and right superior vena cava, Fontan connection, hepatic veins, azygos vein, and the pulmonary arteries. Virtual surgery was performed on the patient-specific 3D model to reflect the planned surgical options. Multiple software tools were utilized to perform the virtual surgery including 3-Matic (Materialise), 3DEXPERIENCE (Dassault Systemes), and Autodesk Netfabb (Autodesk). The primary goal in each patient was to achieve balanced HVF to the 2 lungs. The cardiac surgeon for each patient worked with an engineer (NS or EE) on the 3D modeling team to plan the virtual surgery and reviewed the virtual surgery models prior to computational modeling.

CENTRAL ILLUSTRATION **3-Dimensional Modeling Workflow With Computational Fluid Dynamic Simulation for Planning Fontan Surgery**

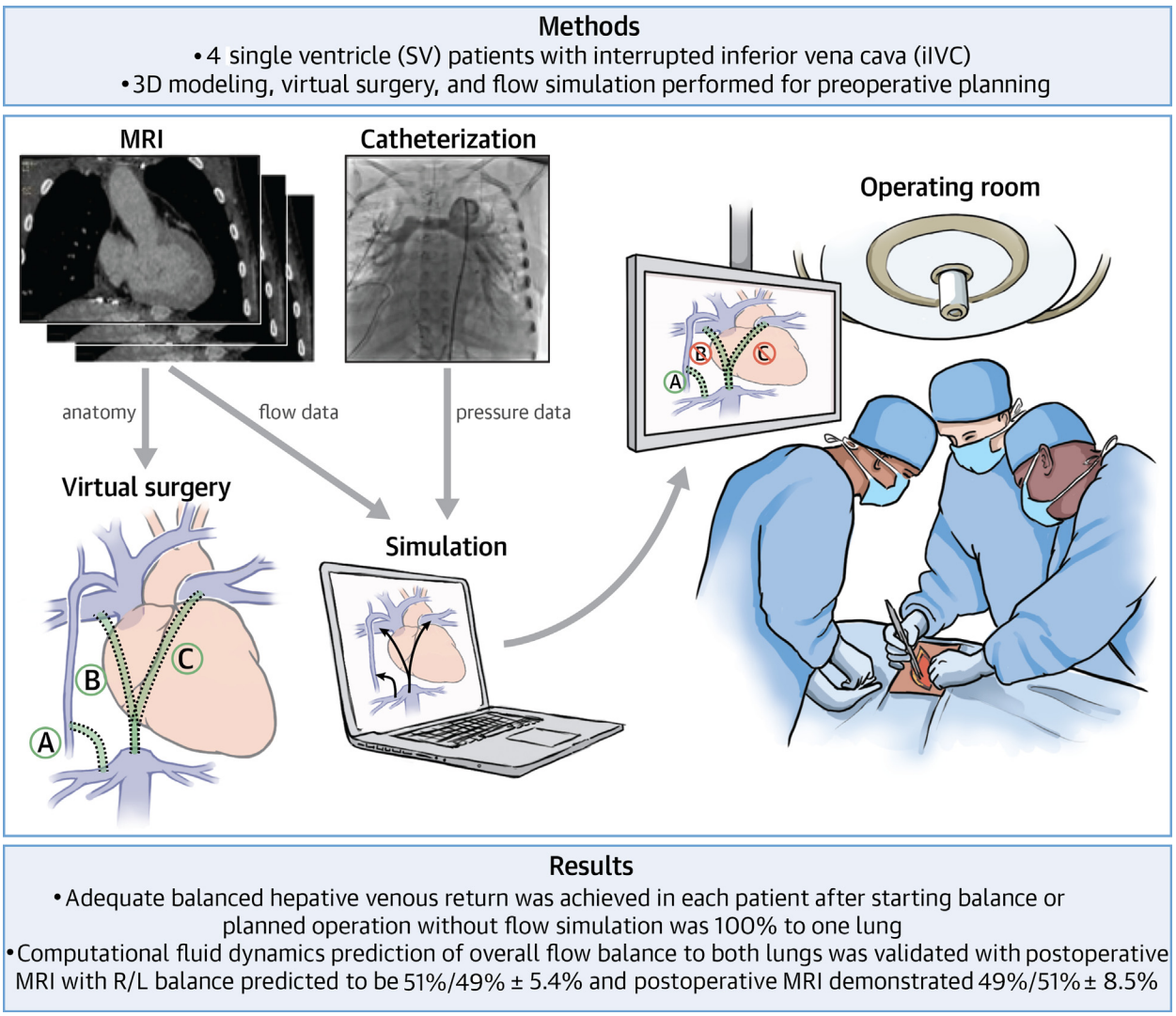

Hoganson DM, et al. JACC Adv. 2024;3(7):101057.

A prospective 3D modeling workflow with computational fluid dynamic simulation of surgical options for Fontan completion or revision with balanced hepatic venous return for preoperative planning and intraoperative guidance. 3D = 3-dimensional; MRI = magnetic resonance imaging; R/L = right/left.

CFD ANALYSIS. Assessment of blood flow in the current anatomy was accomplished with CFD analysis using the patient-specific 3D model. The expected blood flow after surgery was calculated utilizing CFD analysis of the different virtual surgery models for each patient.

Blood flow was simulated in pre- and post-op anatomies by solving the incompressible Navier-Stokes equation using the commercial CFD software, ANSYS Fluent R17.2 (ANSYS).[1] In our CFD simulations, blood was assumed as a Newtonian fluid with a viscosity of 3.5 cP and a density of 1,060 kg/m^3. More detail of our solution process is provided in the Supplemental Appendix. Numerical convergence of our quasisteady simulations was achieved by setting a convergence criterion of 10^{-6} for continuity and velocity, and the solution was iterated until convergence for each time step. A total simulation time of 10 s was carried out for each simulation during which a steady state solution was achieved. All our

TABLE 1 Baseline Clinical Characteristics of Interrupted IVC Patients Undergoing Fontan Completion or Fontan Revision

	Prospective Patients			
	P1	**P2**	**P3**	**P4**
Diagnosis	Heterotaxy (polysplenia), dextrocardia, {A,L,L} DORV, RdAVC, iIVC bilateral SVC	Heterotaxy (polysplenia) with CAVC, iIVC with azygos continuation to LSVC, bilateral SVC	Heterotaxy with {A,D,D} DORV with LdAVC, iIVC with azygos continuation	Heterotaxy, {A,D,D} TGA/VSD, bilateral SVC, iIVC with azygos continuation to LSVC
Age (y)	4.0	9.3	18.0	13.4
BSA (m^2)	0.63	0.98	1.75	1.16
SVC anatomy	Bilateral	Bilateral	Single LSVC	Bilateral
Surgical stage	Bilateral BDG-Kawashima	Fontan completion	Fontan completion	Fontan completion
AVM presence	No evidence	Left lung	Left lung	Left lung
AVM grade	None	Macro	Micro	Micro
Baseline O_2 saturation (%)	88	86	91	91
Left pulmonary vein O_2 saturation (%)	97	68	86	83
PA pressures (mm Hg)	11	17	16	18

simulations were carried out in the Orchestra (O2) high-performance computing cluster managed by the Harvard Medical School.

To accurately model blood flow in the Fontan, patient-specific hemodynamic factors (boundary conditions) were applied to the boundaries of the model. Pre-op MRI was utilized to obtain the flow from the SVC, IVC, and hepatic veins. 4D flow MRI is the standard pre-operative clinical imaging utilized for our 3D modeling workflow involving simulations. In addition to measuring the flows in all involved vessels, we also utilized the phasic inflow of the inferior vena cava and hepatic veins in the boundary conditions for the model. The flow in individual hepatic veins was measured by MRI, and the individual hepatic veins are included in the 3D model geometry. There was streaming of individual hepatic veins[24] within Fontan conduits[25] that could substantially influence the predicted hepatic blood flow distribution. Assuming laminar axial hepatic vein flow at the Fontan inlet is an oversimplification that omits important details in hepatic blood flow. Pulmonary artery pressure was modeled as a static pressure (n = 3) or as a constant hydraulic resistance (n = 1) utilizing the catheterization data for each patient.

It has been shown previously that blood flow, particularly hepatic blood flow, can be reduced under anesthesia.[26,27] As catheterization and MRI or CT data

FIGURE 1 Computational Flow Modeling Workflow

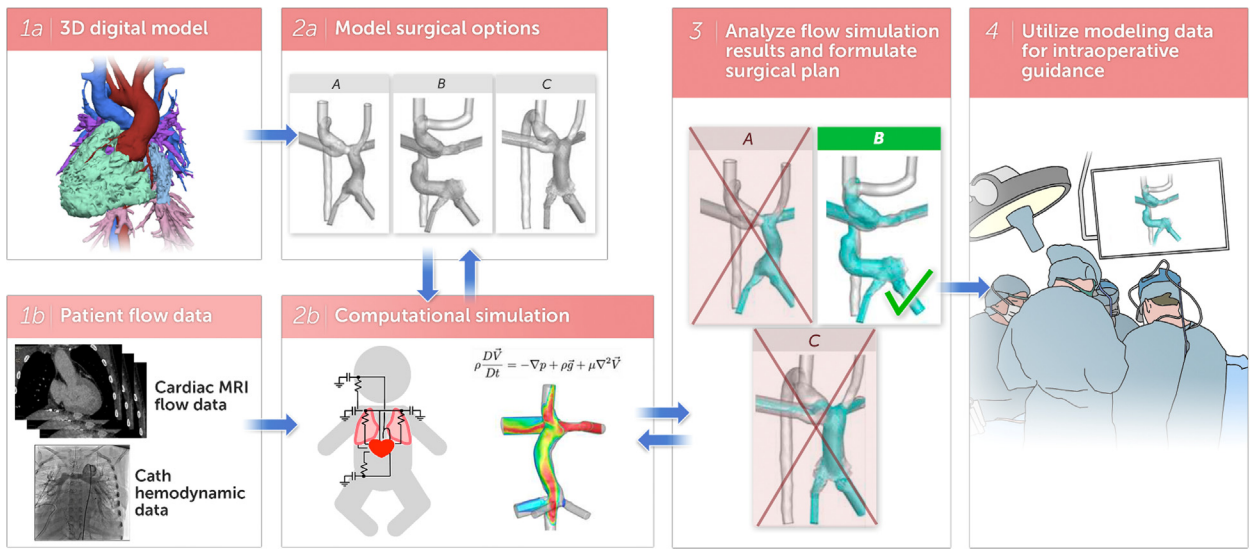

FIGURE 2 Boundary Conditions for Computational Flow Modeling

A

Anesthesia (MRI)	Normal	Post-prandial	Exercise
Q_{in}^{LSVC}, Q_{in}^{RSVC}, Q_{in}^{AZ}	1.5× MRI	1.5× MRI	3× MRI
Q_{in}^{HR}	1.5× MRI	3× Normal	1.5× MRI
Q_{in}^{HL}	1.5× MRI	3× Normal	1.5× MRI

B

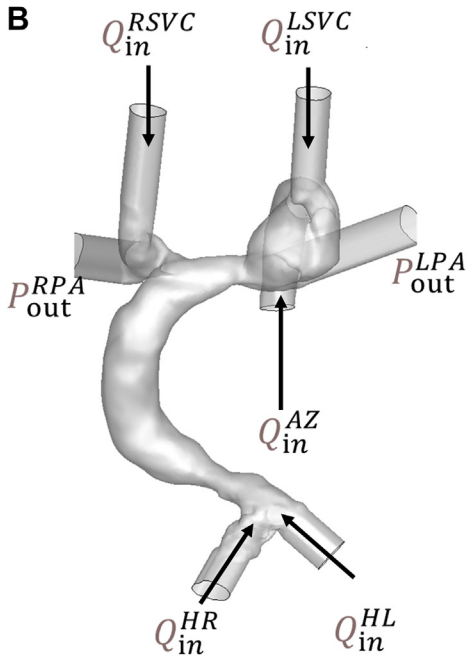

	MRI (Anesthesia)
Q_{in}^{LSVC}	0.86 l/min
Q_{in}^{RSVC}	1.89 l/min
Q_{in}^{AZ}	1.28 l/min
Q_{in}^{HR}	0.085 l/min
Q_{in}^{HL}	0.085 l/min
P_{out}^{LPA}	17 mmHg
P_{out}^{RPA}	17 mmHg

C

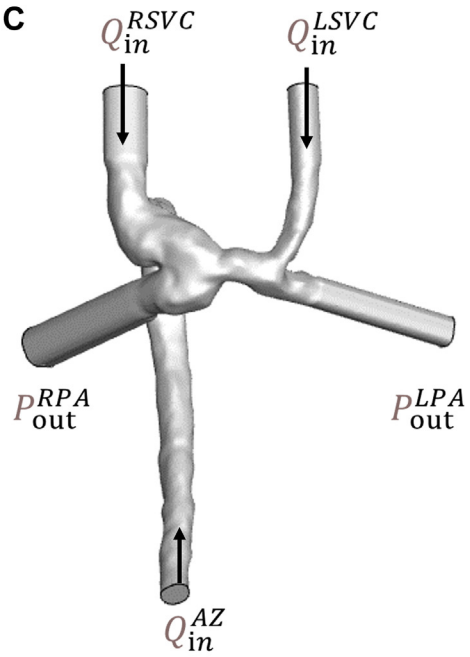

	MRI (Anesthesia)
Q_{in}^{LSVC}	0.63 l/min
Q_{in}^{RSVC}	0.58 l/min
Q_{in}^{AZ}	1.23 l/min
P_{out}^{LPA}	LPM
P_{out}^{RPA}	LPM

(A) Boundary conditions for acquired MRI flow data and relative increases in flow for simulated normal physiologic condition, postprandial condition, and exercise condition. (B) Patient-specific boundary conditions for patient P1. (C) Patient-specific boundary conditions for patient P2.

in these subjects were acquired under anesthesia, performing the simulations using only boundary conditions obtained during anesthesia would not accurately reflect the normal physiologic states of these patients. To predict the robustness of each surgical option to achieve balanced HVF in normal physiology, we simulated 4 flow states: anesthetized, baseline resting stage termed "normal", postprandial, and exercise. This is a critical improvement over prior simulation approaches for Fontan circulation to evaluate how robust the solutions will be for real life, not just for the physiology under anesthesia. Here, normal flow conditions were simulated by assuming a 1.5-fold increase in the hepatic vein inflow rates

FIGURE 3 Computational Fluid Dynamics Results for Patient P1 Including as Bidirectional Glenn and Multiple Simulated Surgical Options for Fontan Completion

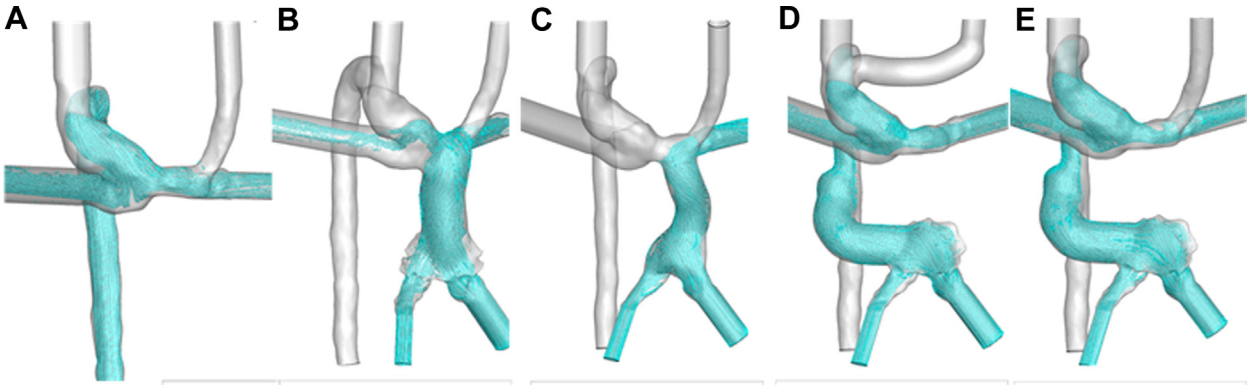

Physiologic Condition	Hepatic Venous Blood Flow (%)		Hepatic Venous Blood Flow (%)		Hepatic Venous Blood Flow (%)		Hepatic Venous Blood Flow (%)	
	RPA	LPA	RPA	LPA	RPA	LPA	RPA	LPA
Anesthesia	03	97	0	100	42	58	46	54
Normal	11	89	0	100	41	59	52	48
Post-prandial	02	98	0	100	77	23	78	22
Exercise	05	95	0	100	33	67	51	49

(A) Baseline flow as bilateral Glenn circulation. (B) Lateral tunnel Fontan. (C) Extracardiac Fontan. (D) Hepatoazygos shunt with the creation of neo-innominate vein and ligation of left superior vena cava. (E) Hepatoazygos shunt.

compared to the conditions under general anesthesia which is a conservative approximation consistent with published data of 2-fold increase in hepatic venous flow in Fontan patients under general anesthesia versus awake;[27] postprandial conditions were simulated by increasing the hepatic vein flow by 3-fold over the normal flow conditions to evaluate the robustness of the Fontan anatomy for higher hepatic venous flow which is 2× higher than published increase in postprandial blood flow in non-Fontan children and adults;[28] and finally, exercise flow conditions were simulated by increasing SVC and azygos inflow by 2-fold over normal flow conditions. **Figure 2A** highlights the boundary conditions for the 4 patients over the 4 different physiologic states. These simulations performed under different inflow conditions allowed prediction of how parameters of interest (ie, hepatic flow distribution, energy loss, and wall shear stress) varied across different flow conditions for a given surgical plan. The boundary conditions for 2 patients are shown in **Figures 2B and 2C** with the additional patients shown in Supplemental Figures 1 and 4.

QUANTIFYING HEPATIC VENOUS BLOOD FLOW DISTRIBUTION. To quantify HVF distribution, massless particles were uniformly seeded at the hepatic vein inlets and were passively carried along with the flow. These particles were tracked and their flux quantified as they exited the PA outlets.[16,21] The equations utilized for particle flux can be found in the Supplemental Appendix.

POWER LOSS CALCULATION. In SV palliation such as Fontan completion or HA shunting, systemic venous return to the pulmonary circulation involves passive flow. In these circulations, favorable flow dynamics involving minimal energy loss is highly desirable as abnormal flow (eg, boundary layer separation leading to vortex roll-up) is often associated with increased energy loss.[25,29] Energy loss has been used as an important hemodynamic parameter in several studies involving analysis of total cavopulmonary circulation.[20,29-31] In our model, power loss was calculated as described in[29] and is available in the Supplemental Appendix.

ITERATIVE CHANGES TO VIRTUAL SURGERY MODELS AND REPEAT CFD ANALYSIS. In all patients, initial surgical reconstruction proposed by the surgeon and cardiologist to balance or rebalance HVF to both lungs did not result in an acceptable balance. A manual iterative refinement of the geometry was part of the workflow, including a review of the CFD results, modification of the operative plan to improve

FIGURE 4 Computational Fluid Dynamics Results for Patient P2 Including as Lateral Tunnel Fontan With All Hepatic Venous Flow Directed to the R Lung and Multiple Simulated Surgical Options for Fontan Revision

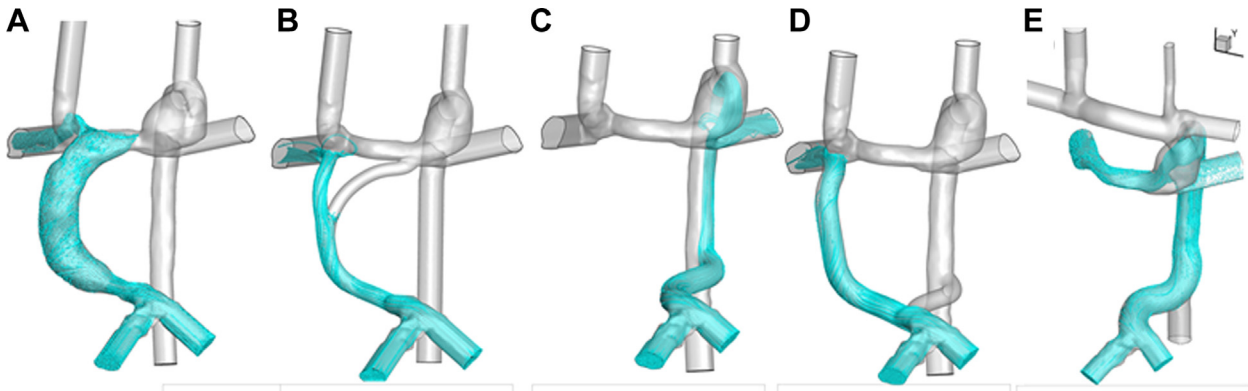

Physiologic Condition	A: Hepatic Venous Blood Flow (%)		B: Hepatic Venous Blood Flow (%)		C: Hepatic Venous Blood Flow (%)		D: Hepatic Venous Blood Flow (%)	
	RPA	LPA	RPA	LPA	RPA	LPA	RPA	LPA
Anesthesia	100	0	0	100	100	0	25	75
Normal	100	0	0	100	100	0	30	70
Post-prandial	100	0	0	100	100	0	58	42
Exercise	100	0	0	100	100	0	18	82

(A) Baseline flow as lateral tunnel Fontan. (B) Y-graft Fontan. (C) Hepatoazygos shunt. (D) Hepatoazygos shunt with additional extracardiac Fontan conduit to right pulmonary artery. (E) Hepatoazygos shunt with the creation of neo-innominate vein and ligation of right superior vena cava.

hepatic flow balance, and creation of new virtual surgery 3D models. This workflow resulted in several different surgical models created for each patient until an acceptable balance of HVF was achieved.

RESULTS

Overall, an iterative workflow was developed to create patient-specific 3D models, perform virtual surgery, and evaluate surgical options with CFD utilizing patient-specific hemodynamics over multiple physiologic states. This workflow resulted in a plan for achieving balanced HVF to both lungs in 4 prospectively evaluated patients.

The virtual surgical options that were created and their resulting HVF distributions for a prospectively evaluated patient (Patient P1) prior to Fontan are shown in **Figure 3**. A standard Fontan completion would have resulted in 100% of HVF to the left lung. Modeling predicted that an HA shunt (3E) would achieve balanced HVF, and the patient successfully underwent that operation.

Shown in **Figure 4** are the virtual surgical options and corresponding HVF distributions in a prospectively evaluated Fontan patient (Patient P2) who, preoperatively, had 100% of HVF going to the right lung and AVMs in the left lung. Multiple surgical options were evaluated, including a Y graft, HA shunt, and combination of Y graft and HA shunt. None of these had adequately balanced HVF over a range of physiologic conditions. However, an HA shunt with surgical construction of an innominate vein achieved stable balance of HVF and the patient successfully underwent that operation. The details of the 2 additional patients can be found in **Supplemental Figures 2 and 3**.

Postoperative validation of simulation results was performed by MRI in all patients. As there are no clinically available MRI approaches to measure HVF distribution specifically, the validation efforts focused on the overall distribution of pulmonary blood flow to the right and left pulmonary arteries. The CFD models predicted a right/left pulmonary artery flow balance of 51%/49% ± 5.4%, and the post-op MRI demonstrated a right/left pulmonary artery flow balance of 49%/51% ± 8.5%. **Table 2** shows the changes in oxygen saturations including the post-intervention L pulmonary venous saturations in each of the patients and the status of their pulmonary AVMs at mean follow-up of 2.5 ± 0.52 years. There was improvement in oxygen saturations and improvement or resolution of AVMs in all Fontan

TABLE 2 Follow-up Clinical Characteristics of Interrupted IVC Patients Undergoing Fontan Completion or Fontan Revision

	Prospective Patients			
	P1	P2	P3	P4
Baseline O_2 saturation (%)	88	86	91	91
Most recent O_2 saturations (%)	97	86	93	94
Most recent AVMs	none	mild +	mild	none
PA pressures (mm Hg)	13	20	12	16
Left pulmonary vein O_2 saturation (%)	N/A	78	92	N/A
Years after intervention	2	2.75	1.92	2.75

revision patients with the exception of patient 2 who was diagnosed with Abernethy syndrome over 2 years after her Fontan revision. She did have improvement in her left pulmonary vein saturations, but overall systemic saturations were not improved.

The power-loss predicted for the Fontan completion or revision procedures at normal physiology were low at 24 ± 1 mW. The postprandial and exercise power loss were scaled up as expected at 27 ± 3 and 75 ± 6 mW.

DISCUSSION

iIVC patients have a wide range of anatomical variations that pose a challenge for planning and predicting the ideal surgical reconstruction for Fontan completion. Prospective virtual modification of patient anatomy to simulate a surgical approach combined with computational modeling provided insight to the physiologic impact of different surgical decisions. One patient required analysis of 4 different surgical approaches and over 80 simulations to determine the best predicted surgical approach. In every patient, there was a substantial change, based upon the computational modeling, in the initial surgical plan proposed by the patient's surgeon and cardiologist. Three of the 4 modeled patients were rescue patients or patients who already had undergone a Fontan and had marked HVF maldistribution with substantial decrease in saturations because of AVM formation. Given variation of the hepatic venous flow balance in the retrospective patients, as well as the experience of other investigators who have done flow simulation for iIVC patients, it is clear that it is not possible to predict HVF distribution based on clinical experience alone, even at large centers with substantial experience with these patients. The drivers of HVF distribution include position of the systemic veins (side of single SVC or bilateral SVC), the side of the azygos vein, and angulation of the veins as they enter the pulmonary arteries and the momentum that results, the flow balance between different vena cava, and other hemodynamic factors. These complex factors make it impossible to accurately predict the best HVF balance from visual estimation or clinical experience. An HA shunt should be considered in all patients with iIVC and azygos continuation, but that alone is not the solution for every patient. The conclusion from our experience is that computational modeling to evaluate and optimize the surgical approach for Fontan completion should be considered in all SV patients with iIVC and azygos continuation, with the goal of ensuring HVF balance, minimizing power loss, and avoiding development of AVMs.

The hemodynamic boundary condition information for CFD was gleaned from catheterization and 4D flow MRI studies, which are typically performed under anesthesia. Performing CFD analysis with only the boundary conditions obtained under anesthesia has the potential to generate misleading results as the patients spend their lives at normal resting conditions, exercising, and during/after eating. For all patients, we performed the simulations for the baseline anatomy and different virtual surgical procedures with 4 hemodynamic conditions—anesthetized and scaled blood flow to represent normal resting physiology, postprandial physiology with increased hepatic venous return, and exercise with increased SVC and azygos flow (**Figure 2**, Supplemental Figure 1). Evaluating surgical options at these different conditions gives a picture of the robustness of the surgical options. This is a critical concept as there can be substantial differences in HVF distribution among these different physiologic conditions as highlighted in **Figures 3 and 4**. The chosen surgical approach resulted in balanced HVF under all simulated physiologic conditions. Future efforts to refine the inlet-specific scaling factors for each physiologic condition will be important to continue to optimize the analyses. As the primary goal is the balance of HVF to the right and left lungs, it would be ideal if this could be calculated in 4D flow MRI. Although there are groups working on this, it is not yet clinically available.

Validation of blood flow simulation results with 4D flow MRI is essential and is performed on every patient where CFD was utilized in clinical decision-making. The congruence between the predicted overall right and left pulmonary artery blood flow and the postoperative blood flow measured by MRI was excellent in this group with essentially no difference observed. This is a combination of the effectiveness of the patient-specific boundary conditions applied and the surgery being performed in accordance with the surgical plan outlined with the modeling effort.

Close collaboration between the modeling team engineers and the surgeons is essential to translate details of the surgeons' planned operative approach into the virtual model. The 3D models of the planned reconstruction are displayed in a monitor in the operating room using the Mimics Viewer software (Materialize) and can be rotated and manipulated to guide the surgeon in the reconstruction.

STUDY LIMITATIONS. The number of subjects analyzed was small. Many important factors of Fontan physiology are not currently accounted for in the computational models including the impacts of breathing and gravity. Breathing will be incorporated in future studies in a formal way at the level of the modulation of pulmonary vascular resistance in a frequency and amplitude that varies for the different physiologic states that are routinely tested in our methods. However, incorporation of phasic flow from 4D flow MRI improves the fidelity of the input boundary condition of the SVC and IVC over assuming steady state flow[23] and does directly incorporate much of the patient-specific breathing hemodynamics impacts as that is a major driver of the phasic flow variation. The complexities of pulmonary vascular resistance may not be completely captured by the lumped parameter model although it is an improvement over utilizing pulmonary artery pressures alone. Future work on measuring the complex impedance of the pulmonary vasculature in SV patients and further understanding the relative flow rates in normal resting, exercise, and postprandial conditions would be further steps to improve the fidelity of the simulation. The minimum amount of hepatic venous return to one lung to prevent AVM's is unknown but may be in the 10 to 20% range. This is a subject of future investigation to further improve the target range for hepatic venous return balance.

CONCLUSIONS

SV patients with iIVC have complex physiology, and determining the best surgical approach can be challenging. Patient-specific 3D models, prospective virtual surgery, and CFD analysis over several physiologic states predicts HVF distribution to the lungs in order to optimize the surgical plan. This computational workflow may avoid HFV maldistribution and the subsequent formation of pulmonary AVMs.

FUNDING SUPPORT AND AUTHOR DISCLOSURES

Gift in-kind software from Dassault Systemes. All other authors have reported that they have no relationships relevant to the contents of this paper to disclose.

ADDRESS FOR CORRESPONDENCE: Dr David M. Hoganson, Harvard Medical School, Boston Children's Hospital, 300 Longwood Ave, Mail Stop BCH 3084, Boston, Massachusetts 02115, USA. E-mail: David.Hoganson@cardio.chboston.org.

PERSPECTIVES

COMPETENCY IN MEDICAL KNOWLEDGE: SV patients with iIVC and azygos continuation are at risk for formation of pulmonary AVMs after Fontan completion due to the complexity of achieving balanced return of hepatic venous flow to both lungs. A 3D modeling workflow with CFD simulation of surgical options of Fontan completion can predict hepatic venous blood flow distribution to preoperatively optimize the surgical approach to reduce the risk of AVM formation.

TRANSITIONAL OUTLOOK 1: Multiphysiologic state CFD analysis with scaled flow based on MRI obtained under anesthesia predicts the hepatic venous and total pulmonary blood flow distribution for real life physiology, and further MRI testing of single ventricle patients under different physiologic states will continue to advance this critically important approach.

TRANSITIONAL OUTLOOK 2: CFD accurately predicts total pulmonary blood flow distribution as validated by post-op MRI in Fontan patients. Future MRI techniques will also be able to measure hepatic venous flow distribution.

REFERENCES

1. Srivastava D, Preminger T, Lock JE, et al. Hepatic venous blood and the development of pulmonary arteriovenous malformations in congenital heart disease. *Circulation*. 1995;92:1217-1222.

2. Kartik SV, Sasidharan B, Gopalakrishnan A, et al. A comparative study of invasive modalities for evaluation of pulmonary arteriovenous fistula after bidirectional Glenn shunt. *Pediatr Cardiol*. 2021;42:1818-1825.

3. Loomba RS. Arterial desaturation due to pulmonary arteriovenous malformations after the Kawashima operation. *Ann Pediatr Cardiol*. 2016;9:35-38.

4. Setyapranata S, Brizard CP, Konstantinov IE, Iyengar A, Cheung M, d'Udekem Y. Should we always plan a Fontan completion after a Kawashima procedure? *Eur J Cardio Thorac Surg*. 2011;40:1011-1015.

5. Van Galder H, Schaal AM, Feng M, et al. Increases in oxygen saturation following discharge from Fontan palliation - an indicator of resolution of pulmonary arteriovenous malformations? *Cardiol Young*. 2021;31:1807-1813.

6. Alibrahim IJ, Mohammed MHA, Kabbani MS, et al. Pulmonary arteriovenous malformations in children after the Kawashima procedure: risk

factors and midterm outcome. *Ann Pediatr Cardiol*. 2021;14:10–17.

7. Adamson GT, Peng LF, Lui GK, Perry SB. Transcatheter redirection of hepatic venous blood to treat unilateral pulmonary arteriovenous malformations in a Fontan circulation by short-term total exclusion of the unaffected lung. *Catheter Cardiovasc Interv*. 2019;93:660–663.

8. Alsoufi B, Rosenblum J, Travers C, et al. Outcomes of single ventricle patients undergoing the Kawashima procedure: can we do better? *World J Pediatr Congenit Heart Surg*. 2019;10:20–27.

9. McElhinney DB, Kreutzer J, Lang P, Mayer JE Jr, del Nido PJ, Lock JE. Incorporation of the hepatic veins into the cavopulmonary circulation in patients with heterotaxy and pulmonary arteriovenous malformations after a Kawashima procedure. *Ann Thorac Surg*. 2005;80:1597–1603.

10. McRae RO, Lambert LM, Williams RV, Martin MH, Burch PT. Modification of hepatic venous conduit to manage pulmonary arteriovenous malformations. *World J Pediatr Congenit Heart Surg*. 2015;6:477–479.

11. Sundareswaran KS, de Zelicourt D, Sharma S, et al. Correction of pulmonary arteriovenous malformation using image-based surgical planning. *JACC Cardiovasc Imaging*. 2009;2:1024–1030.

12. Wu IH, Nguyen KH. Redirection of hepatic drainage for treatment of pulmonary arteriovenous malformations following the Fontan procedure. *Pediatr Cardiol*. 2006;27:519–522.

13. Arrigoni SC, van den Heuvel F, Willems TP, et al. Off-pump hepatic to azygos connection via thoracotomy for relief of fistulas after a Kawashima procedure: ten-year results. *J Thorac Cardiovasc Surg*. 2015;149:1524–1530.

14. Montesa C, Karamlou T, Ratnayaka K, Pophal SG, Ryan J, Nigro JJ. Hepatic vein incorporation into the azygos system in heterotaxy and interrupted inferior vena cava. *World J Pediatr Congenit Heart Surg*. 2019;10:330–337.

15. Ahmed Y, Tossas-Betancourt C, van Bakel PAJ, et al. Interventional planning for endovascular revision of a lateral tunnel fontan: a patient-specific computational analysis. *Front Physiol*. 2021;12:718254.

16. de Zelicourt DA, Haggerty CM, Sundareswaran KS, et al. Individualized computer-based surgical planning to address pulmonary arteriovenous malformations in patients with a single ventricle with an interrupted inferior vena cava and azygous continuation. *J Thorac Cardiovasc Surg*. 2011;141:1170–1177.

17. de Zelicourt DA, Kurtcuoglu V. Patient-specific surgical planning, where do we stand? the example of the fontan procedure. *Ann Biomed Eng*. 2016;44:174–186.

18. Frieberg P, Aristokleous N, Sjoberg P, Toger J, Liuba P, Carlsson M. Computational fluid dynamics support for fontan planning in minutes, not hours: the next step in clinical pre-interventional simulations. *J Cardiovasc Transl Res*. 2021;15:708–720.

19. Haggerty CM, de Zelicourt DA, Restrepo M, et al. Comparing pre- and post-operative Fontan hemodynamic simulations: implications for the reliability of surgical planning. *Ann Biomed Eng*. 2012;40:2639–2651.

20. Haggerty CM, Kanter KR, Restrepo M, et al. Simulating hemodynamics of the Fontan Y-graft based on patient-specific in vivo connections. *J Thorac Cardiovasc Surg*. 2013;145:663–670.

21. Trusty PM, Wei ZA, Slesnick TC, et al. The first cohort of prospective Fontan surgical planning patients with follow-up data: how accurate is surgical planning? *J Thorac Cardiovasc Surg*. 2019;157:1146–1155.

22. van Bakel TMJ, Lau KD, Hirsch-Romano J, Trimarchi S, Dorfman AL, Figueroa CA. Patient-specific modeling of hemodynamics: supporting surgical planning in a fontan circulation correction. *J Cardiovasc Transl Res*. 2018;11:145–155.

23. Wei ZA, Huddleston C, Trusty PM, et al. Analysis of inlet velocity profiles in numerical assessment of fontan hemodynamics. *Ann Biomed Eng*. 2019;47:2258–2270.

24. Rijnberg FM, van der Woude SFS, van Assen HC, et al. Non-uniform mixing of hepatic venous flow and inferior vena cava flow in the Fontan conduit. *J R Soc Interface*. 2021;18:20201027.

25. Rijnberg FM, Hazekamp MG, Wentzel JJ, et al. Energetics of blood flow in cardiovascular disease: concept and clinical implications of adverse energetics in patients with a fontan circulation. *Circulation*. 2018;137:2393–2407.

26. Gelman SI. Disturbances in hepatic blood flow during anesthesia and surgery. *Arch Surg*. 1976;111:881–883.

27. Caro-Dominguez P, Chaturvedi R, Chavhan G, et al. Magnetic resonance imaging assessment of blood flow distribution in fenestrated and completed fontan circulation with special emphasis on abdominal blood flow. *Korean J Radiol*. 2019;20:1186–1194.

28. Muthusami P, Yoo SJ, Chaturvedi R, et al. Splanchnic, thoracoabdominal, and cerebral blood flow volumes in healthy children and young adults in fasting and postprandial states: determining reference ranges by using phase-contrast MR imaging. *Radiology*. 2017;285:231–241.

29. Restrepo M, Tang E, Haggerty CM, et al. Energetic implications of vessel growth and flow changes over time in Fontan patients. *Ann Thorac Surg*. 2015;99:163–170.

30. Ding J, Liu Y, Wang F. Influence of bypass angles on extracardiac Fontan connections: a numerical study. *Int J Numer Method Biomed Eng*. 2013;29:351–362.

31. Trusty PM, Wei Z, Tree M, et al. Local hemodynamic differences between commercially available Y-grafts and traditional fontan baffles under simulated exercise conditions: implications for exercise tolerance. *Cardiovasc Eng Technol*. 2017;8:390–399.

KEY WORDS 3D model, flow modeling, Fontan, single ventricle, virtual surgery

APPENDIX For supplemental methods and figures, please see the online version of this paper.